Electronic Supplementary Material (ESI) for Journal of Materials Chemistry C.


# Supporting Information

## A Hybrid 3D Printing for Highly-efficient Nanoparticle Micropatterning

Sayli Jambhulkar[a], Dhraneedhar Ravichadran[a], Barath Sundaravadivelan[b], Kenan Song[*c]

[a] *Systems Engineering, The School of Manufacturing Systems and Networks (MSN), Ira A. Fulton Schools of Engineering, Arizona State University (ASU), Mesa, AZ, USA 8521*

[b] *Mechanical Engineering, The School for Engineering of Matter, Transport and Energy (SEMTE), Ira A. Fulton Schools of Engineering, Arizona State University (ASU), Tempe, AZ, USA 85287*

[c] *The School of Manufacturing Systems and Networks (MSN), Ira A. Fulton Schools of Engineering, Arizona State University (ASU), Mesa, AZ, USA 85212*

[*] *Corresponding author, Email: kenan.song@asu.edu*

## Table of content:

**Table of Figures:**



**Table of Tables:**

## Experimental Section

### *Materials*

Titanium Aluminum carbide ($Ti_3AlC_2$) MAX (≥90%, ≤40 μm particle size, CAS-No 196506-01-1, Sigma Aldrich, USA), hydrochloric acid (ACS reagent, 37%, CAS-No 7647-01-0, Sigma Aldrich, USA), lithium fluoride (98.5%, CAS-No 7789-24-4, Alfa Aesar, USA), De-ionized water (CAS-No 7732-18-5, Sigma Aldrich, USA), acrylonitrile butadiene styrene (ABS) 3D printing filament (diameter of 1.75 mm, glass transition temperature (Tg) ≈105°C, density ≈1.06 gm/cc, CAS-No 9003-56-9, product No 3DXABS011, Sigma Aldrich, USA), and ethanol (anhydrous, ≥99.5%, Sigma Aldrich, USA, CAS-No 64-17-5) were used in this research. All chemicals were used as received without further purification.

### *MXene synthesis*

The $Ti_3AlC_2$ MAX (400 mesh) powders were purchased from Sigma Aldrich of 38 μm particle size. For in-situ HF etching, 1 gm of $Ti_3AlC_2$ MAX power was slowly added into the etchant mixture of lithium fluoride (1 gm) and 9M hydrochloric acid and then stirred continuously at 500 rpm for 24 hr at 35°C. After the completion of etching, the exfoliated MXene nanoparticles mixture was washed several times with DI water (The clear acidic supernatant was discarded, and DI water was added again) via centrifugation (3500 rpm 15 mins for each cycle) until the neutral pH (i.e., pH ≈7) of the supernatant was obtained. The sediment clay was dispersed in 50 ml deaerated water and delaminated by sonication under flowing Ar for 30 min. The obtained suspension was centrifuged at 3500 rpm for 40 min, and the stable MXene colloidal solution as the supernatant was collected, which was then vacuum filtered through a PVDF membrane. Finally, the dried MXene flakes were dispersed in ethanol for further NPs deposition and patterning study.

### *FDM 3D printing*

The pure ABS filament was 3D printed via a Flashforge 3D printer (i.e., the model is Creator 3 Pro) to prepare the template of various topologies (e.g., LH, microchannel dimensions, surface roughness) (**Fig. 1a**). The 3D model consisting of a rectangular substrate (20x5 mm) and a reservoir (2x2 mm) (**Fig. 1a$_1$**) was prepared by SolidWorks software and exported as an STL file for FDM 3D printing. FlashPrint was used to conduct the digital slicing of the 3D model. First, the object was sliced in the direction parallel to the long edge of the substrate (x-y plane) and perpendicular to the reservoir (z-axis), followed by 3D printing in a layer-upon-layer fashion to create the microchannels connecting to the reservoir. Multiple samples were printed before optimizing the 3D printing parameters. The following 3D printing parameters were used: nozzle diameters 0.4 mm, LH 20-400 μm, nozzle temperature 235° C, print bed temperatures 110° C, print speed 60 mm/sec, and infill percentage 100 %.

### *MXene nanoparticle deposition*

The 5 and 10 mg/ml concentration MXene ink was prepared by dispersing the NPs in ethanol by sonication for 15 minutes. Then the stable ink was loaded into the DIW syringe, and a single drop of approximately 5 μl volume was deposited into the 3D printed reservoir (**Fig. 1b**). After the drop deposition in a reservoir, the dispersion would be confined within the microchannels and driven via capillary action following ethanol evaporation at room temperature (RT) (i.e., controlled by drying thermodynamics with the total time for deposition and evaporation ≈10 sec for 2 cm microchannels) (**Fig. 1b$_1$**). After the solvent evaporation, whether the mono- and multilayer microstructure of MXene NPs formed directed assembly within the microchannels would depend on DIW processing parameter control (e.g., the number of deposition layers) and printing ink characteristics (e.g., particle size, colloidal rheology).

### *Characterization*

The scanning electron microscope (SEM) images and energy dispersive spectroscopy (EDS) mapping were measured by vacuum field-emission SEM (FE-SEM) (Auriga, SE, 5-20 kV). X-ray diffraction (XRD) spectra were obtained from a PAN analytical X'Pert PRO powder diffractometer in the range of 5–70° (2θ) with a step size of 0.01°. The interlayer spacing (d) of multilayered MXene was calculated according to the following Bragg's law equation.[1]

$$d = \frac{\lambda}{2sin\theta} \qquad \textbf{Equation S1}$$

Here, $\lambda$ is the wavelength of the X-ray source (i.e., 1.54 Å), and $\theta$ is the scattering angle of the (002) peak.

The optical imaging, 3D surface imaging, height profile, and surface roughness of the FDM-printed substrates and MXene-deposited thin films were taken from the Keyence optical scanning microscope. In addition, atomic force microscopy (AFM) images were captured by Witech Alpha 300 RA in tapping mode with 8 nm tip radius.

The rheology test of MXene dispersion was conducted using TA instruments (Discovery HR2) rheometer with a 40 mm 2° (truncation gap ≈ 60 μm) cone Peltier plate. The viscoelastic properties of the MXene dispersion were studied by measuring the viscosity, viscous modulus (G'), and elastic modulus (G") of the sample as a function of frequency (i.e., 1 to 100 Hz) at a constant stress of 0.015 Pa at RT.

***Ansys simulation***

An Ansys Fluent simulation was done for the 5 mg/ml MXene concentration solution. The physical properties such as density (5 mg/cc), viscosity (0.002 Pa/s), capillary pressure, and capillary force values were given as calculated from the experimentation (**Table S1**). The reservoir size (l x b x d = 900 x 80 x 80 μm) and the length of the grooves (2 cm) were kept constant for all the samples, while the width and depth of the groves were changed for different samples similar to the as-printed substrates for different LH. A volume of a fluid system with an explicit solution method and a laminar model was considered. The boundary conditions were set as close to the actual experimental values to replicate the capillary action of the MXene solution transport. The simulation was run at a time step of 0.05 sec for 20 sec. It was observed that the sample with the smallest groove dimension had the least ink transport compared to higher groove dimensions.

**Table S1.** Approximate value of microfluid forces acting on MXene NPs during fluidic deposition

| Symbol | Microfluidic forces | Equation | Value (N) | Ref. |
|---|---|---|---|---|
| $F_{c1}$ | Capillarity for the ink liquid | $\gamma * 2cos\theta * w * 0.5$ | 1.14 x $10^{-6}$ | 2,3 |
| $F_{d1}$ | Drag Force | $½ (C_D * \rho * A_C * v_1^{2}$ | 5.73 x $10^{-16}$ | 4 |
| $F_{d2}$ | Drag Force | $½ (C_D * \rho * A_C * v_2^{2}$ | 7.23 x $10^{-21}$ | 4 |
| $F_g$ | Gravitational Force | $V * \Delta\rho * g$ | 5.9 x $10^{-17}$ | 5 |
| $F_{vdw}$ | vander Waal's Force | - | 0.5-2.5 x $10^{-11}$ | 6 |
| $F_{c2}$ | Microcapillary Force between NPs | - | 1-25 x $10^{-8}$ | 7 |

**Table S2.** The approximate values of capillary force ($F_c$) and Reynold's number (Re) of MXene ink within microchannels of different LH, aspect ratio, and microchannel angle ($\alpha=\tan^{-1}(2D/W)^{\circ}$)

| LH | $F_c$ (N) | $Re_{ink}$[8] | Aspect ratio (D/W) | $\alpha$[9] |
|---|---|---|---|---|
| **50** | 0.49*$10^{-6}$ | 0.0078 | 0.23 | 24.70 |
| **100** | 1.14*$10^{-6}$ | 0.016 | 0.26 | 27.47 |
| **150** | 1.71*$10^{-6}$ | 0.023 | 0.27 | 28.36 |
| **180** | 2.55*$10^{-6}$ | 0.027 | 0.35 | 34.99 |

- $F_{c1}$ is the dominant force that initiates the motion of MXene/ethanol suspension from the reservoir into the microchannel.
- $F_{d1}$ is the drag force exerted on NPs to transport the ink into the microchannels.
- $F_{d2}$: The drag force MXene particles are dragged toward the pinned meniscus by convection which is opposing the sedimentation can be ignored ($F_g$>$F_{d2}$).
- $F_g$ is a gravitational force that promotes the sedimentation of MXene NPs for layer-by-layer deposition in between the walls of microchannels after ethanol evaporates.
- $F_{vdw}$: After the evaporation of ethanol, particles form closely assembled in-between the microchannel due to Van der Waal's attraction force.
- $F_{c2}$: The sedimented NPs experience Laplace pressure gradient and pulled together by micro-capillary forces when they are closer in the range of a few 10's or 100's of nm.

**Calculation of Microfluidic Forces:**

**1. The capillary force acting on fluid ($F_{c1}$)**[2,3]

$$F_c = 2 * \gamma * \left(\frac{cos\ \theta}{w/2}\right) * (0.5 * D * W)$$

**Equation S2**

Here,
θ = 15.5°= Contact angles for ethanol with the ABS substrate
W= width of the microchannel =LH
D= depth of the microchannels
$\gamma$ = surface tension between the ethanol and air = 22.39 mN/m
A= crosssectional area of microchannels = 0.5*W*D
For LH = 100
As per Young Laplace equation P is capillary pressure
$F_C$= P x A = 22.39 x $10^{-3}$ x ((2 x 0.963)/(100/2) x $10^{-6}$) x 0.5 x 26.33 x $10^{-6}$ x 100 x $10^{-6}$ = 1.14 x $10^{-6}$ N

**2. Reynold's number for fluid**

$$Re = \frac{\rho\ u\ D_H}{\mu}$$

**Equation S3**

Here,
ρ= density of ethanol = 789.2 kg/$m^3$
u= fluid velocity in microchannels = 0.3 mm/s (5 mg/ml)
$D_h$=Width of microchannels = W
μ= viscosity of the ink = 0.0015 Ns/$m^2$ (5 mg/ml)
For LH = 100
Re= (789.2 x 0.1 x $10^{-3}$ x 100 x $10^{-6}$)/0.0025 = 0.016

**3. Drag Force ($F_{d1}$ & $F_{d2}$)**

$$F_d = ½\ (C_D * \rho * A_C * v^2)$$

**Equation S4**

$$F_{d1} = ½\ (C_D * \rho * A_C * v_1^2)$$ (Fluid flow into the channel)

$$F_{d2} = ½\ (C_D * \rho * A_C * v_2^2)$$ (Sedimentation)

Here,
$C_D$ = Coefficient of drag for flat disc (13.6/Re for parallel) and (20.4/Re for perpendicular) to flow [7]
ρ= density of particle = 4000 kg/$m^3$
$A_c$ = Area of cross-section of particles = 500 nm x 7.5 nm
$v_1$= velocity of fluid = 0.3 x $10^{-3}$ m/sec
$v_2$ = velocity of particles during sedimentation = 26.33 μm/30 sec =0.87 x $10^{-6}$ m/sec
$F_{d1}$= 0.5 x 555 x 4000 x 500 x $10^{-9}$ x 7.5 x $10^{-9}$ x (0.3 x $10^{-3}$)$^2$ = 5.73 x $10^{-16}$ N
$F_{d2}$= 0.5 x 832 x 4000 x 500 x $10^{-9}$ x 7.5 x $10^{-9}$ x (0.87 x $10^{-6}$)$^2$ = 7.23 x $10^{-21}$ N

**4. Sedimentation Force ($F_g$)**

$$F_g = V * \Delta\rho * g$$

**Equation S5**

Here,
V = volume of nanoparticle = 500 x 500 x 7.5 x $10^{-27}$ $m^3$
$\Delta\rho = \rho_{particle} - \rho_{fluid}$ = 4000-789.2 kg/$m^3$
g = acceleration due to gravity = 9.81 m/$s^2$
$F_g$= (500 x 500 x 7.5 x $10^{-27}$) x 3210.8 x 9.81 = 5.9 x $10^{-17}$ N

**5. Peclet Number**[11]

$$Pe = \frac{6\pi\mu\,\dot{\gamma} r_p^3}{k_B T}$$ = 2.71

Where,
γ is shear rate = 24 1/s
$k_B$ is Boltzmann constant = 1.308649 × 10 J/K
T is temperature =298 K
μ is viscosity if ink = 0.0015 Pa.s
$r_p$ is nanoparticle radius = 250 nm

Pe >1 means the fluid transport is convective controlled and NPs are primarily being transported by the bulk fluid flow rather than by molecular diffusion.

**6. Stokes Number**[12]

$$S_t = \frac{\rho_p d_p^2\, U_0}{18\mu D}$$ = 1.38x10-4

Where,
$\mu$ is viscosity of fluid = 0.0015 kg/m.s
$\rho_p$ is the density of particle = 5 mg/ml
$D_p$ is particle diameter = 500 nm
$U_0$ is velocity of fluid = 0.3 mm/s
D is the diameter if the channels = 100 μm

St << 1 means suspended NPs are well dispersed in fluid and follows fluid streamlines.

**7. Characteristic sedimentation time** is measured as 10-15 sec.

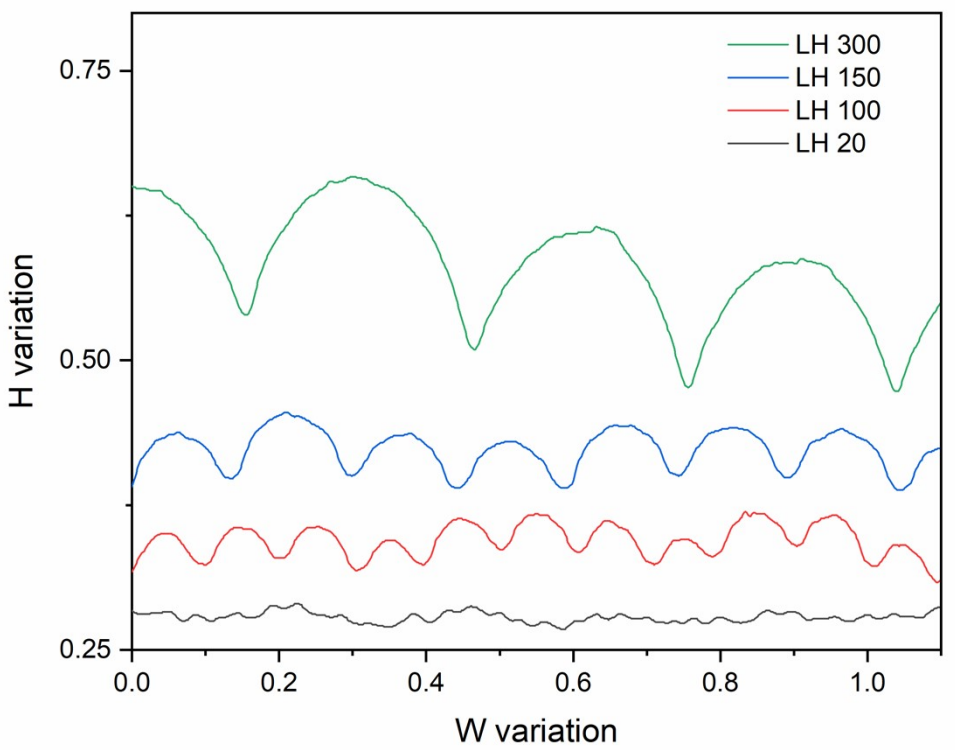


**Fig. S1.** Height profile generated on the surface of 3D printed template for different LH.

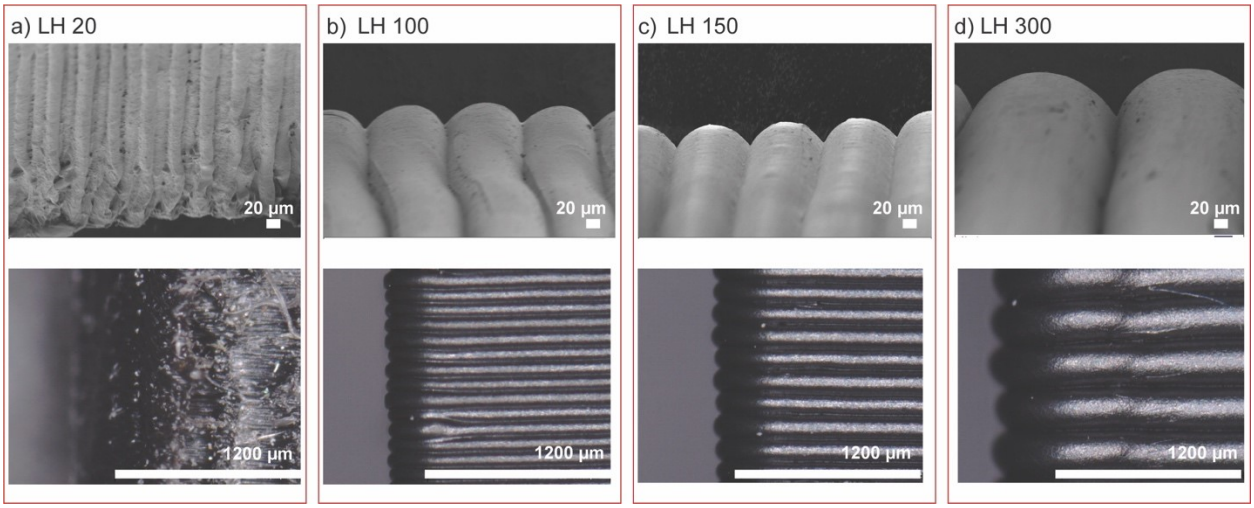


**Fig. S2.** SEM and optical images of a cross-sectional view of 3D printed templates demonstrating stairstep topology for a) LH 20 µm, b) LH 100 µm, c) LH 150 µm, d) LH 300 µm

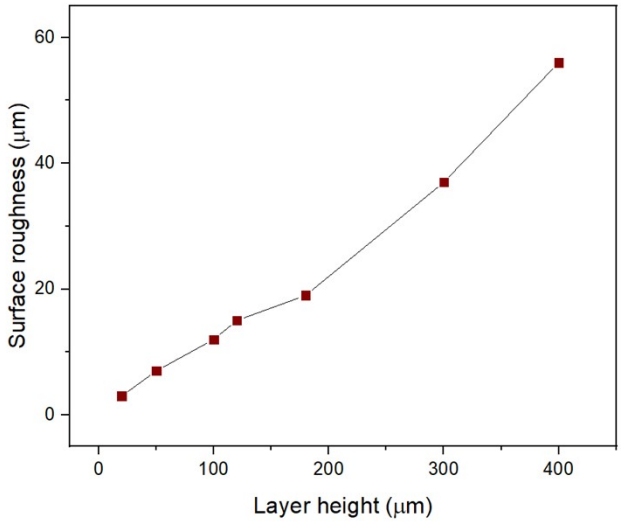


**Fig. S3.** Average surface roughness ($S_a$) generated on the 3D printed template surface for different LH

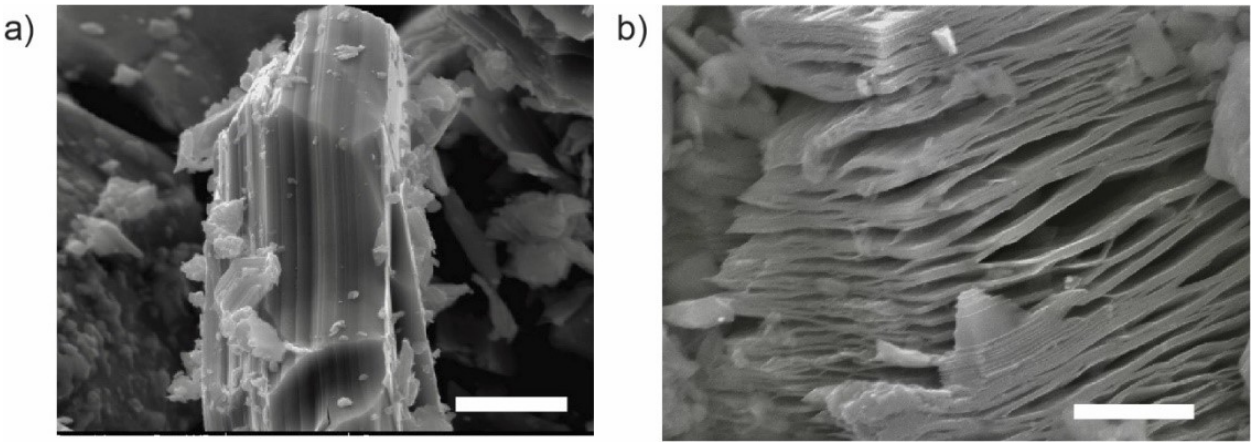


**Fig. S4.** a) $Ti_3AlC_2$ MAX particle morphology with the characteristic layered structure (Scale bar 2 μm), b) MXene particles after etching show accordion structure (Scale bar 1 μm)

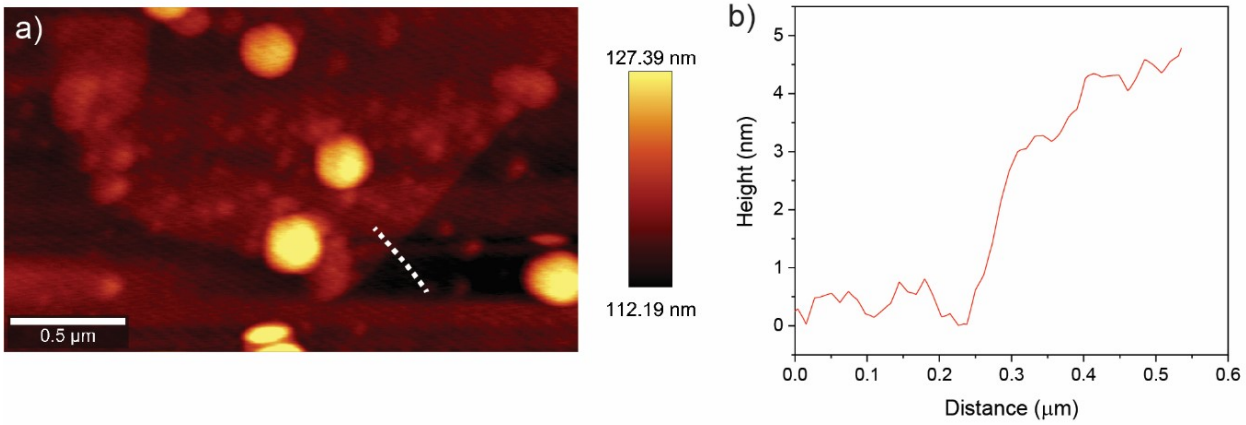


**Fig. S5**. a) AFM image of MXene flake obtained by drop casting on a $SiO_2$ substrate and b) its height profile.

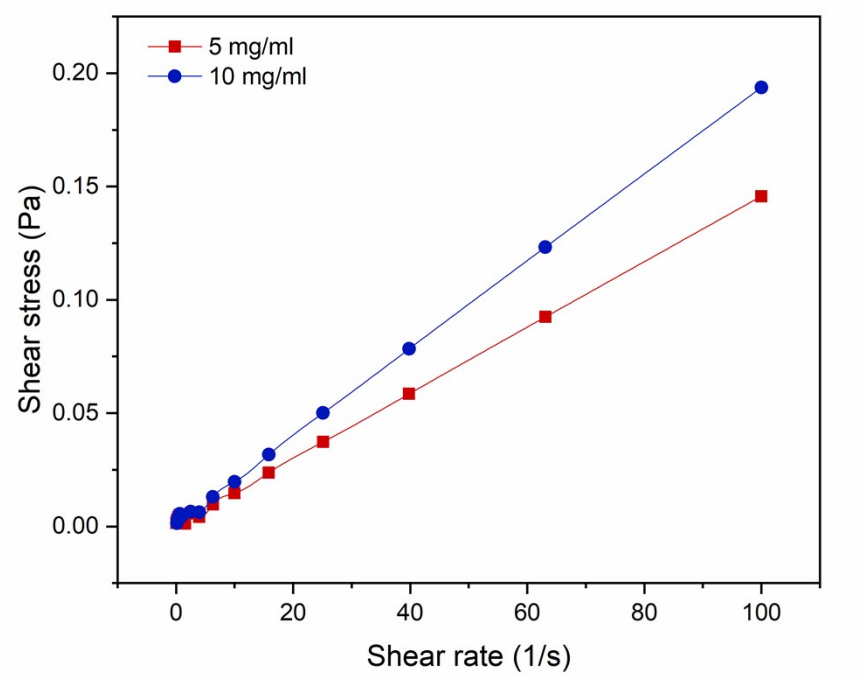


**Fig. S6.** Shear stress as a function of shear rate for MXene/ethanol inks.

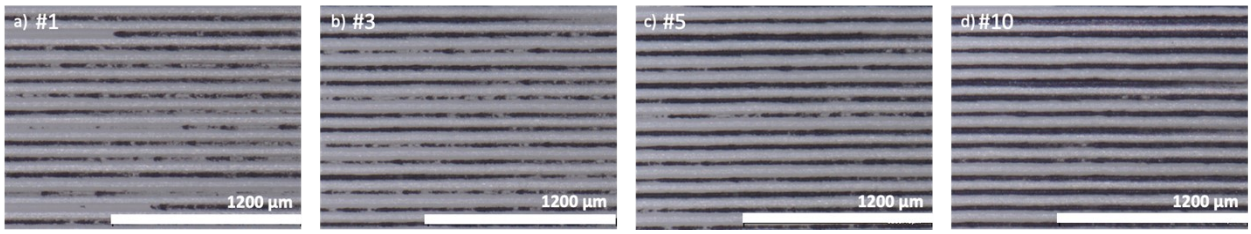


**Fig. S7.** MXene/ethanol ink (5 mg/ml) deposited in microchannels by DIW with one single droplet of 5 µL as one deposition cycle for different numbers of deposition cycles (#n).

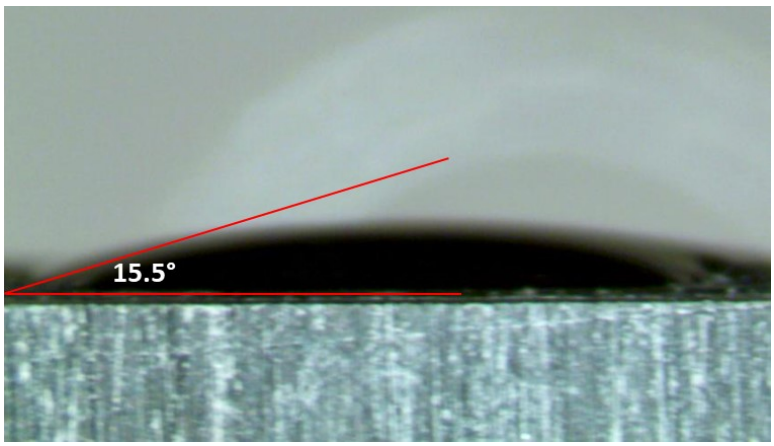


**Fig. S8.** The measured static contact angle between ethanol and flat ABS surface.

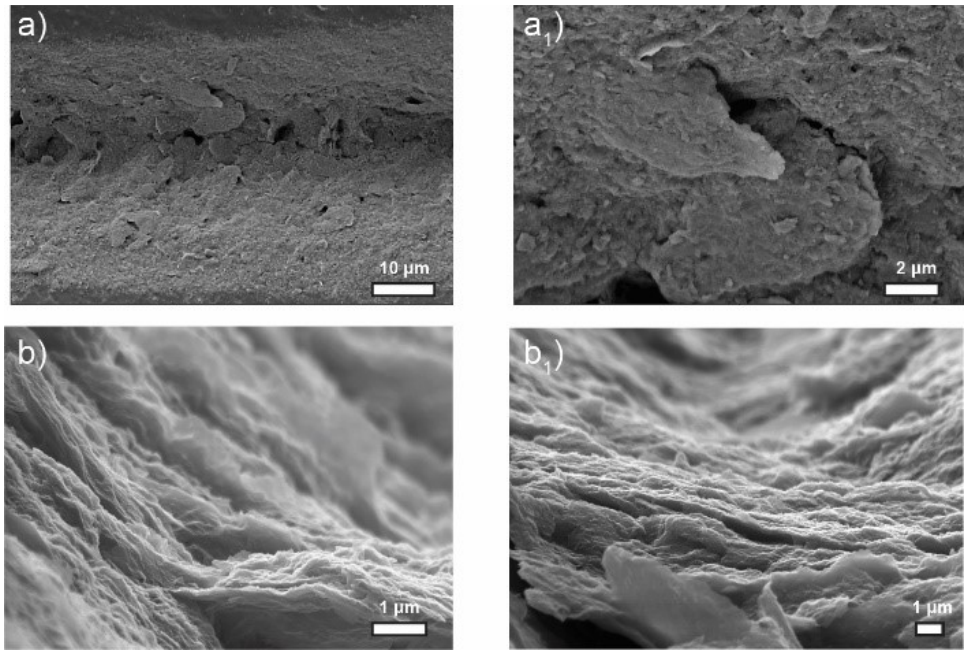


**Fig. S9.** SEM images of the a) top view of the patterned MXene film at microchannel with continuous morphology and b) parallelly stacked MXene flakes for 5 mg/ml #5.

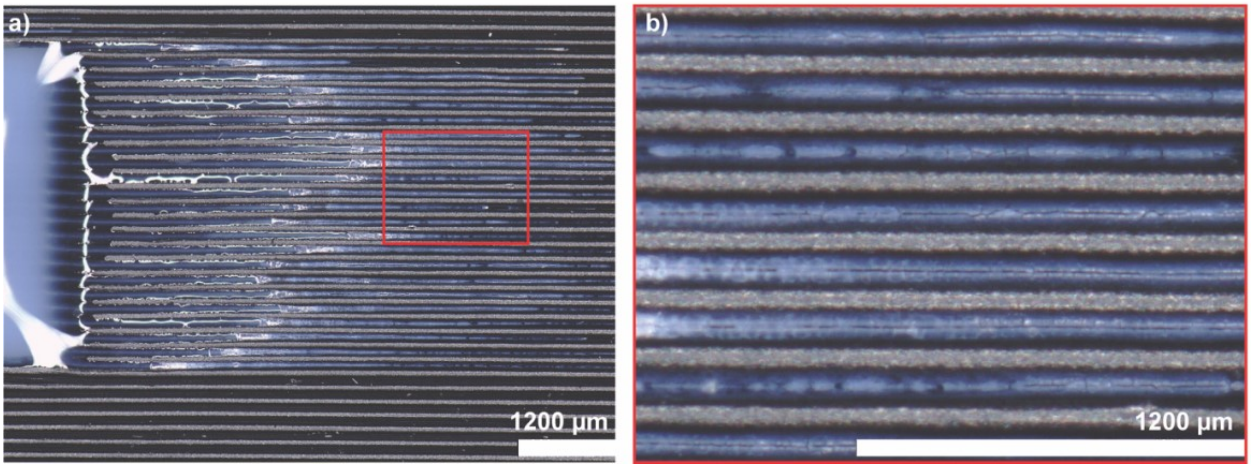


**Fig. S10.** Microfluidic deposition of 1D NPs (i.e., halloysite nanotubes in ethanol 1mg/ml) into microchannels by capillary action.

**References:**


1 J. Epp, in *Materials Characterization Using Nondestructive Evaluation (NDE) Methods*, Elsevier, 2016, 81–124.
2 J. R. Fanchi, *Principles of applied reservoir simulation*, Gulf Professional Pub, Amsterdam, 2008, 27-44.
3 D. Tiab and E. C. Donaldson, *Petrophysics theory and practice of measuring reservoir rock and fluid transport properties*, Gulf Professional Pub, Boston, 2008, 297-316.
4 C. Gissler, S. Band, A. Peer, M. Ihmsen and M. Teschner, *Computers & Graphics*, 2017, **69**, 1–11.
5 H. Chanson, *The hydraulics of open channel flow: an introduction: basic principles, sediment motion, hydraulic modelling, design of hydraulic structures*, Elsevier Butterworth-Heinemann, Amsterdam, 2004, 21-26.
6 S. Antonyuk, *Particles in Contact: Micro Mechanics, Micro Process Dynamics and Particle Collective*, Springer International Publishing Imprint, Springer, Cham, 2019, 239-276.
7 J. N. Israelachvili, *Intermolecular and surface forces*, Elsevier, Academic Press, Amsterdam, Third edition., 2011, 107-130.
8 J. Happel and H. Brenner, *Low Reynolds number hydrodynamics*, Springer Netherlands, Dordrecht, 1981, **1**, 23-57.
9 H. Wang, M. He, H. Liu and Y. Guan, *Materials Today Physics*, 2021, **20**, 100461.
11 B. Kim, S. S. Lee, T. H. Yoo, S. Kim, S. Y. Kim, S.-H. Choi and J. M. Kim, *Sci. Adv.*, 2019, **5**, eaav4819.
12 T. L. Chan, J. Z. Lin, K. Zhou and C. K. Chan, *Journal of Aerosol Science*, 2006, **37**, 1545–1561.